ISSN 0036-0236, Russian Journal of Inorganic Chemistry, 2023, Vol. 68, No. 4, pp. 487–495. © Pleiades Publishing, Ltd., 2023.
ISSN 0036-0236, Russian Journal of Inorganic Chemistry, 2023. © Pleiades Publishing, Ltd., 2023.
Russian Text © The Author(s), 2023, published in Zhurnal Neorganicheskoi Khimii, 2023, Vol. 68, No. 4, pp. 560–568.

INORGANIC MATERIALS AND NANOMATERIALS

New Method for Preparation of Composite Based on Montmorillonite and Graphene Oxide

Yu. V. Ioni[a, *], I. V. Sapkov[a, b], S. I. Chentsov[c], E. I. Efremova[a, d, e], and S. P. Gubin[a]

[a] *Kurnakov Institute of General and Inorganic Chemistry, Russian Academy of Sciences, Moscow, 119991 Russia*
[b] *Moscow State University, Moscow, 119991 Russia*
[c] *Lebedev Physical Institute, Russian Academy of Sciences, Moscow, 119991 Russia*
[d] *Lomonosov Institute of Fine Chemical Technologies, MIREA—Russian Technological University, Moscow, 119571 Russia*
[e] *Moscow Aviation Institute (National Research University), Moscow, 125993 Russia*
**e-mail: Acidladj@mail.ru*

Received November 14, 2022; revised November 14, 2022; accepted December 1, 2022

Abstract—A new method for preparation of a composite based on graphene oxide and montmorillonite has been proposed. A comparative characteristic of the adsorption rate for montmorillonite, graphene oxide, and a composite based on them is given. It is shown that the composite has the best adsorption properties with respect to methylene blue. The samples have been studied by IR and Raman spectroscopies, SEM, X-ray powder diffraction, and TGA/DTA. The resulting composite material can be widely used as sorbents for organic dyes in an aqueous medium and organic solvents.

Keywords: adsorption capacity, composite material
DOI: 10.1134/S0036023623600296

INTRODUCTION

At present, due to the increased burden on the environment, in particular, severe pollution of rivers and lakes located near large industrial enterprises and cities, the problem of purification of domestic and industrial wastewater is relevant [1–5]. The growth of science-intensive industries leads to a complication of the composition of wastewater, which may contain emulsions and suspensions of particles and suspensions in the submicron and nanoscale range, organic solvents, oils, which complicates their treatment in urban wastewater treatment plants, whose work consists mainly in mechanical and biological cleaning methods [6–9].

Chemical methods of wastewater treatment include sedimentation and co-precipitation methods based on the principles of chemical adsorption [10–12]. The literature contains a large amount of work aimed at developing new generation adsorbents [13–16] and studying the processes accompanying adsorption [15, 16]. Thus, the authors [17] describe the mechanism for obtaining nanosized needle-shaped boehmite powder (AlOOH) by its recrystallization in a subcritical aqueous medium. The synthesized acicular boehmite has a developed specific surface area (136 m^2/g), which makes it possible to recommend it as an adsorbent for the extraction of metals from industrial wastewater [5, 18] and viruses and bacteria from liquid media [19, 20]. It should be noted that the method proposed by the authors [17] is interesting from a scientific point of view, but rather difficult to implement in industry, since it requires sequential thermal and hydrothermal treatment.

Adsorbents based on various clays and clay materials [21–23] are of interest due to their low cost, high reactive specific surface area, hydrophobicity, potential for exchange processes, high content of cations, etc. A similar material is montmorillonite, which has a sandwich structure and consists of two layers of silicon-oxygen tetrahedra and one layer of aluminum-oxygen octahedra with cations introduced into the structure between the layers. In a number of works [24–26], the possibility of independent use of montmorillonite as an adsorbent was considered.

To solve the problems of adsorption from liquid media, it is interesting to use composites based on montmorillonite and graphene oxide. The high adsorption capacity of graphene oxide is achieved due to the large specific surface area and the presence of oxygen-containing functional groups, which allow to increase the selective adsorption capacity [27, 28]. However, films based on graphene oxide are characterized by the following processes: a change in the surface structure over time and the adhesion of monolayers with the formation of large blocks, which leads to a deterioration in the adsorption capacity of the material.

Table 1. Preparation method and composition of samples

Sample no.	Preparation method	Composition
1	Oxidation of commercial graphite by the Hummers method followed by removal of water	Graphene oxide (GO)
2	Commercial	Montmorillonite (Mt)
3	Mixing suspensions based on graphene oxide (GO) and montmorillonite (Mt) in a ratio of 1 : 1 followed by removal of water	Composite based on GO and Mt
4	Mixing suspensions based on graphene oxide (GO) and montmorillonite (Mt) in a ratio of 10 : 1 followed by removal of water	Composite based on GO and Mt

The purpose of this work is to develop a new method for obtaining a composite based on graphene oxide and montmorillonite and to compare the adsorption capacity for organic dyes using methylene blue as an example, both for individual components (graphene oxide, montmorillonite) and for the composite formed.

EXPERIMENTAL

Sample Preparation

Preparation of a dispersion of graphene oxide (GO) (sample 1). A dispersion of GO was prepared by oxidizing commercial graphite manufactured by Sigma Aldrich (fraction 200 μm) according to the modified Hummers method with further sonication (22 kHz, 1 W/cm^3) in water for 30 min [29, 30]. As a result, an aqueous dispersion of GO with a concentration of 5 mg/mL was obtained. Further removal of water from the aqueous GO dispersion leads to the formation of sample **1.**

Sample 2. Purified Na-montmorillonite produced by Kunimine Industries Co. Ltd. (Japan) containing nearly 100% montmorillonite was used as sample **2**.

Preparation of composites based on graphene oxide (GO) and montmorillonite (Mt) (samples 3, 4). To obtain composites based on graphene oxide and montmorillonite, homogeneous aqueous suspensions of each component were prepared separately. To prepare the GO suspension, we used an 8-mL GO dispersion with a concentration of 5 mg/mL preliminarily sonicated for 30 min. To prepare a suspension based on Mt, Mt (40 mg) in the case of sample **3** and Mt (4 mg) in the case of sample **4** were added to distilled water (40 mL). Mt-based suspensions were sonicated for 30 min. The subsequent mixing of the components was also carried out using ultrasonic treatment for 10 min. The resulting homogeneous suspension was placed for 42 days in a dark room without access to ultraviolet rays at a constant temperature of 25°C for slow water evaporation.

Table 1 shows the method of preparation and the phase composition of the samples used in the work.

Sample Study

The phase composition of the obtained samples was identified using a Bruker D8 Advance setup operating in the reflection mode on CuK_α radiation (40 kV, 40 mA, λ = 1.54056 Å) with a scanning step of 4 deg/min.

The surface morphology was studied on a Carl Zeiss Supra 40 scanning electron microscope (Germany). The samples were placed on a holder, which was placed inside a chamber with a vacuum of ~6–10 mbar. The accelerating voltage during imaging in secondary scattered electrons was 1–10 kV, the aperture was 30 μm.

Transmission electron microscopy (TEM) was performed on a JEOL Jem-1011 instrument at an accelerating voltage of 80 kV. The samples were deposited on copper grids coated with a carbon film by ultrasonic sputtering and then placed inside a chamber with a vacuum of ~6–10 mbar.

Raman spectra were measured using an Inspectr R532 portable Raman spectrometer (Russia) as part of an Olympus CX-41 microscope (Japan). A laser beam (wavelength 532 nm) was focused with an objective onto a sample placed on an adjustable stage. The spectrograph ensured the recording of Raman spectra in the range of 150–4000 cm^{-1} with a spectral resolution of 4 cm^{-1}. The images were taken with a ToupCam 5.1 MP digital camera (China) built into the setup. The IR absorption spectra of the samples were recorded on a Bruker Alpha IR Fourier spectrometer with a Platinum ATR attachment in the range 400–4000 cm^{-1}; scanning step 4 cm^{-1}. The obtained Raman and IR spectra were analyzed on the basis of literature and reference data. The visible UV spectrum was recorded on a Hitachi U-5100 spectrophotometer (Japan) in a standard quartz cuvette 1 cm in diameter.

Synchronous thermal analysis of the powders was carried out on a combined Netzsch STA 449 TGA/DSC TGA/DTA/DSC thermal analyzer with a mass spectrometric detector in platinum-rhodium open crucibles at a heating rate of 10 deg/min in a temperature range of 20–1000°C in a stream of conditioned air (60 mL/min). Al_2O_3 was used as a reference.

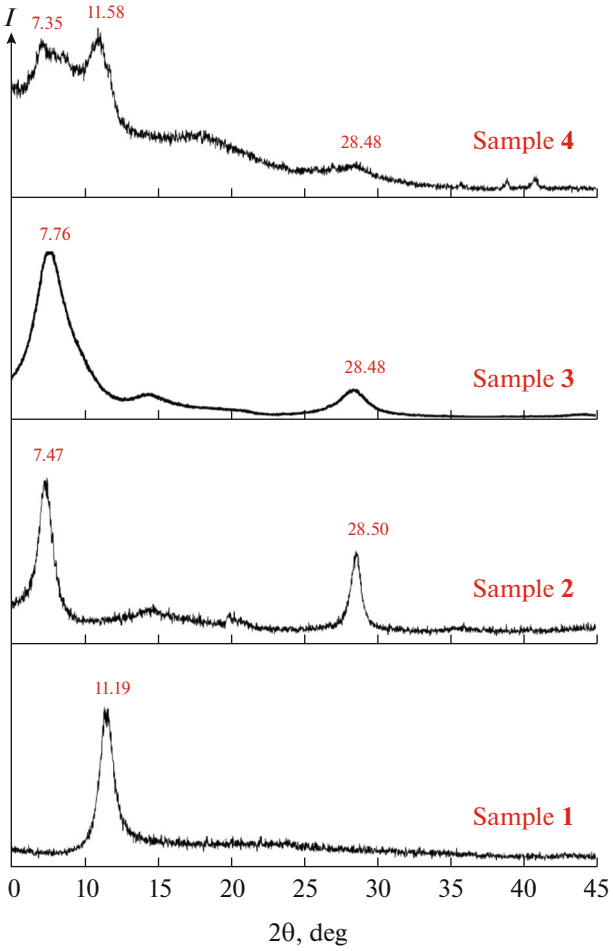

Fig. 1. X-ray diffraction patterns of synthesized samples of graphene oxide, commercial montmorillonite, and composites based on them (samples **1**–**4**).

Methylene Blue Adsorption Study

The studied adsorbent (graphene oxide, montmorillonite, composite based on them (samples **1**–**3**), 10 mg) were placed into a beaker, then a 10 ppm aqueous solution of methylene blue (100 mL) was added. The system was continuously stirred at 1000 rpm. Aliquots of 3 mL were taken at a certain time interval. The taken samples were centrifuged (15000 rpm, 5 min) to separate sorbent particles, and then UV-vis spectra were recorded.

RESULTS AND DISCUSSION

As is known, montmorillonite is a silicate-containing structure of a layered type, consisting of a central octahedral layer of aluminum oxide located between two tetrahedral layers of silicon oxide. Crystal cell parameters of montmorillonite are the following: a_0 = 5.23 Å, b_0 = 9.06 Å, c_0 = 9.6–20.5 Å, $\alpha = \gamma = 90°$, $\beta \sim 100°$, $Z = 2$ [24, 25, 31]. Between the layers of montmorillonite inside the structure, isomorphic substitutions occur, which induce a negative charge, which is naturally balanced by the presence of inorganic cations (Na^+, Ca^{2+}, etc.) or water in the interlayer space and leads to the hydrophilic nature of the substance [31].

Graphene oxide is a nonstoichiometric carbon material with a layered structure and hydrophilic properties [32, 33], which makes it possible to mix Mt and GO suspensions to a homogeneous state, which is achieved by the penetration of Mt particles into GO layers. Ultrasonic treatment of the resulting homogeneous suspension of Mt and GO due to cavitation leads to a coordination interaction between the oxygen-containing functional groups of GO and Mt. The removal of water from the structure and from the surface of Mt and GO is a complex physicochemical process. Of particular note is the formation of surface-bound and internal cluster water in the structure of disperse materials, the removal of which is accompanied by a decrease in the enthalpy of water vaporization [34–36].

The correct sequence of the described manipulations makes it possible to synthesize a composite based on Mt and GO with a thickness of no more than 30 μm.

Figure 1 shows the X-ray powder diffraction patterns of the synthesized samples **1**–**4**. The diffraction pattern of sample **1** contains a reflection corresponding to GO in the region 2θ = 11.58° with an interlayer distance of 7.64 Å calculated using the Bragg formula ($\lambda = 2\sin\theta$). According to [37], the reflection for sample **2** in the region 2θ = 7.47° corresponds to $d(001)$ and indicates a distance of ~11.83 Å between the Mt layers, which can be filled, including with water molecules. The reflections in wider regions 2θ = 28.50° are reflections of the 001 reflection and coincide for samples **2**–**4**. Samples **3** and **4** are characterized by broadening of the reflections at 2θ = 7.76° and 7.35°, which indicates the active inclusion of water molecules in the structure of the synthesized composite. Sample **3** is characterized by the absence of reflections corresponding to the GO phase, which indicates the disordering of the GO structure during the coprecipitation of Mt and GO and the probable penetration of GO monolayers between the Mt layers, which leads to broadening of the Mt reflections in the diffraction patterns. In the case of sample **4**, the X-ray diffraction pattern shows a GO reflection in the region 2θ = 14° during the formation of a composite based on graphene oxide and montmorillonite in a ratio of 10 : 1, which indicates the formation of a dense layered GO structure on the surface of Mt particles with a reduced interlayer distance for GO, which is 7 Å. Based on X-ray powder diffraction, sample **3** was chosen as the most promising for studying the adsorption capacity for organic dyes.

The IR spectroscopy data (Fig. 2a) confirm the X-ray powder diffraction results. The IR spectrum of graphene oxide (sample **1**) contains bands in the

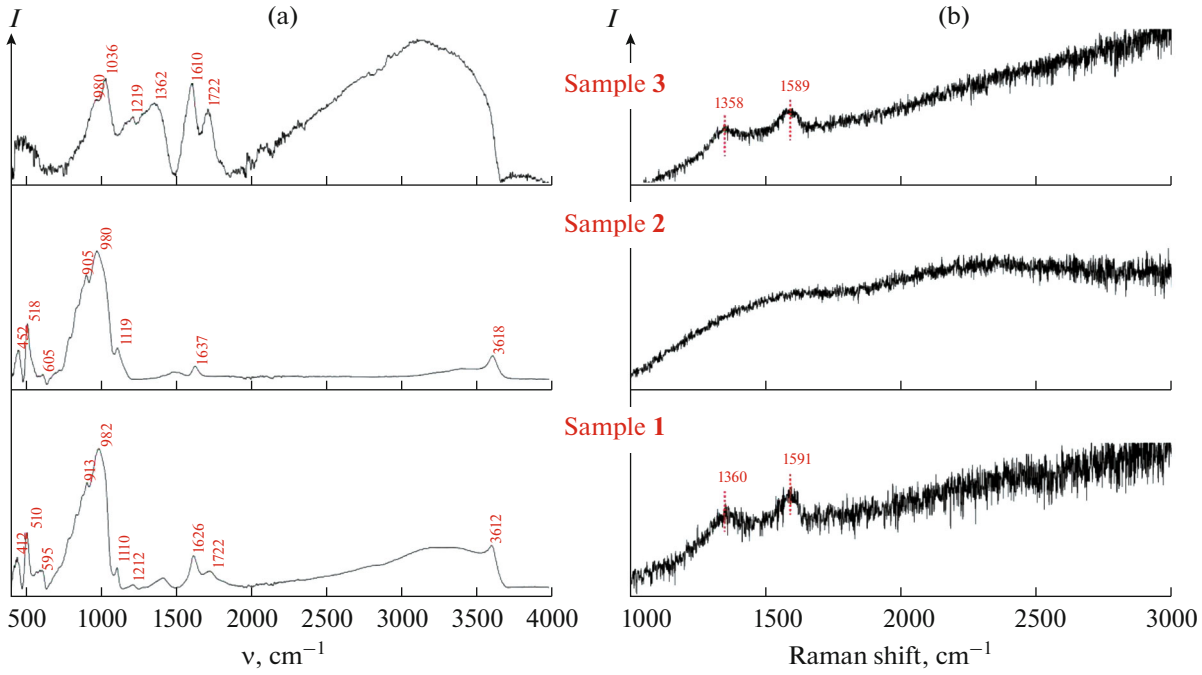

Fig. 2. IR and Raman spectra of synthesized samples **1**–**3**.

region of 1036 cm^{-1} corresponding to the C–O stretching vibrations, at 1219 cm^{-1} assigned to the C–O–C stretching vibrations, at 1362 cm^{-1} assigned to the C–OH bending vibrations, at 1610 cm^{-1} assigned to stretching vibrations of the aromatic system, at 1722 cm^{-1} assigned to the C=O stretching vibrations present at the edges of the GO sheets in the form of carboxyl groups and in lactone groups on the basal plane of GO, and a wide band in the range of 3000–3500 cm^{-1} corresponding to the O–H stretching vibrations, including those from adsorbed water molecules [32, 38, 39]. The IR spectrum of sample **2** (Mt) contains a band at 520 cm^{-1} corresponding to the Si–O–Al stretching vibrations; bands at 600, 976, and 1119 cm^{-1} assigned to the Si–O stretching vibrations, at 905 cm^{-1} assigned to the Al–OH stretching vibrations, at 1637 and 3618 cm^{-1} assigned to the OH stretching vibrations, including those from adsorbed water molecules [24, 34–36]. The IR spectrum of the composite (sample **3**) contains bands characteristic of both graphene oxide and montmorillonite structures. The spectra of samples **3** and **4** almost completely coincide; for convenience, the IR spectrum of sample **3** is shown.

Raman spectroscopy completes data obtained by X-ray diffraction and IR spectroscopy when studying carbon-containing materials. Raman spectrum of sample **1** (Fig. 2b) is characterized by the presence of pronounced bands D (1358 cm^{-1}) and G (1589 cm^{-1}). As is known, band D reflects the degree of disorder of the crystal structure and the decrease in symmetry when the crystal lattice is distorted [39]. The presence of band G is due to in-plane tangential stretching vibrations of carbon atoms in the plane and is observed in the Raman spectrum for all carbon materials with sp^2 bonds. The unoriented Raman spectrum of pure montmorillonite (sample **2**) at 532 nm laser radiation is suppressed by fluorescence. Bands G and D in the spectrum of sample **3** coincide with those in the spectrum of the starting sample **1**, which indicates the invariability of graphene oxide in the synthesized composites. Raman spectra of samples **3** and **4**, containing different amounts of montmorillonite, coincide.

To study the thermal stability up to 1000°C for GO (sample **1**) and a composite based on GO and Mt (sample **3**), studies were carried out by the method of combined TGA/DTA/DSC analysis with a mass spectrometric study of the emitted gaseous products. Figure 3 shows the DTA/TG/DSC curves for sample **1** with exothermic effects: in the range of 100–280°C with a maximum at 178°C, which corresponds to the removal of functional oxygen-containing groups [32] with a weight loss of 30.7%; in the range of 420–700°C with a maximum at 563°C, corresponding to the oxidative pyrolysis of the GO carbon framework with a weight loss of 50.67%. The conclusion about the removal of functional oxygen-containing groups over the entire heating interval to 1000°C is confirmed by mass spectrometry data: a significant release of a gaseous substance with a molecular weight of 44 g/mol (CO_2) is observed. For sample **3** (Fig. 4), the TGA/DTA/DSC curves show three broad exothermic effects. The effect in the range of 120–300°C with a

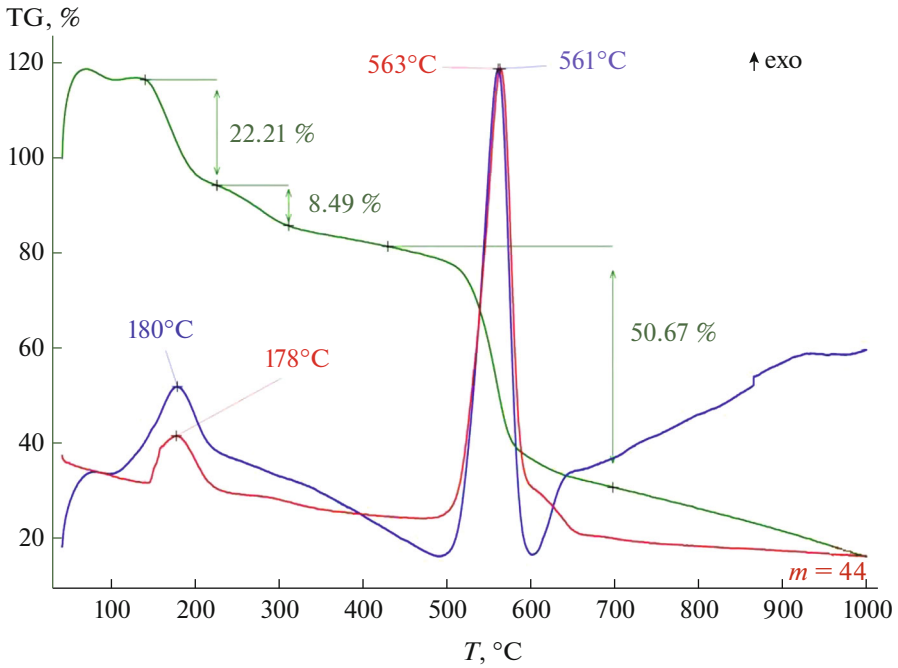

Fig. 3. DTA/TG/DSC curves for sample **1**.

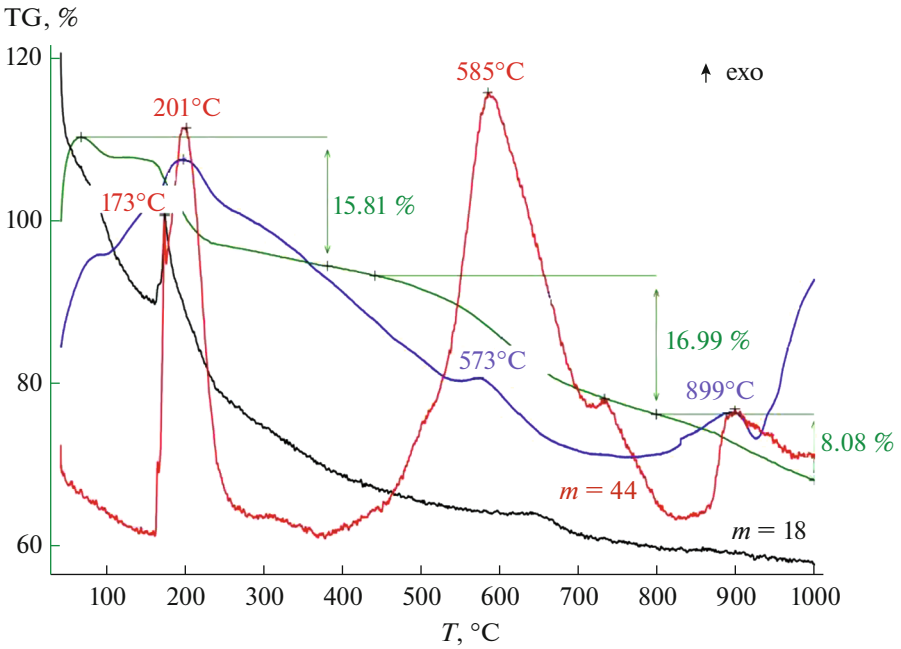

Fig. 4. DTA/TG/DSC curves for sample **3**.

maximum at 201°C is associated with the removal of functional oxygen-containing groups [32] and surface-bound water molecules from the composite structure [34–36] with a weight loss of 14.7%, as evidenced by the presence of effects at 173 and 201°C on the ion current curve for the removal of gaseous substances with a molecular weight of 44 g/mol (CO_2) and 18 g/mol (H_2O). The effect in the range of 500–650°C with a maximum at 585°C corresponds to the oxidative pyrolysis of the GO carbon cage with a weight loss of 14.36%, which is reflected in the ion current curve for the removal of a gaseous substance with a molecular weight of 44 g/mol (CO_2). The effect in the temperature range of 850–950°C with a maxi-

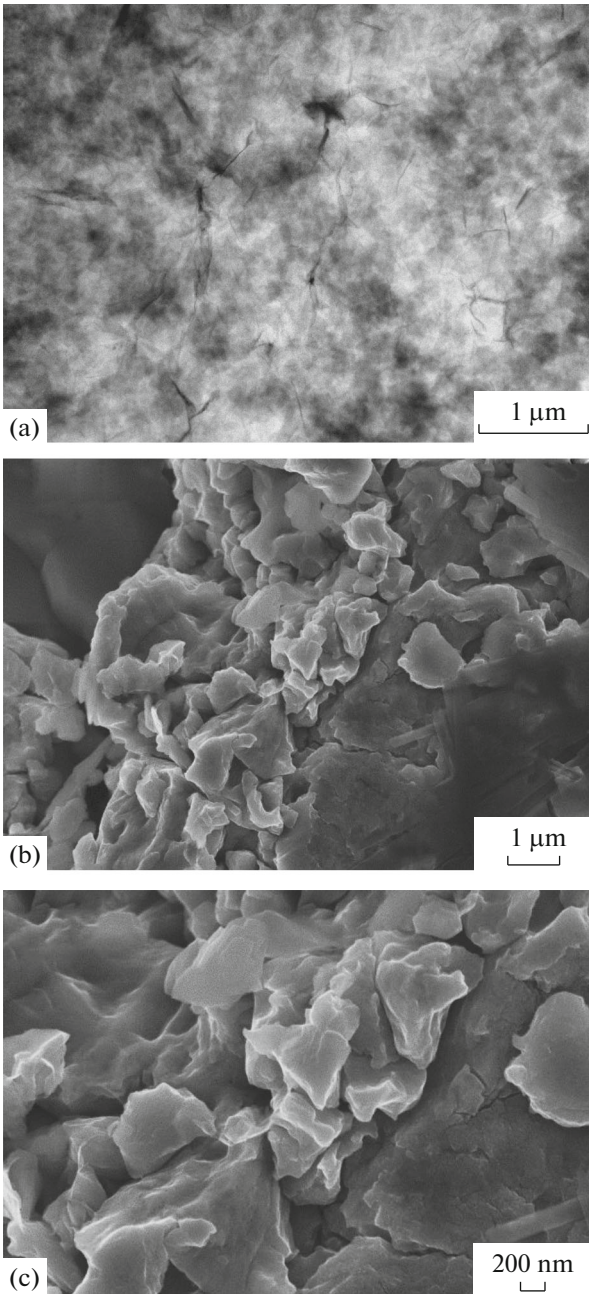

Fig. 5. (a) SEM and (b, c) TEM images of sample **3**.

mum at 899°C corresponds to the destruction of the carbon framework of the GO and Mt composite with a weight loss of 7.01%, which is also reflected in the ion current curve for the removal of a gaseous substance with a molecular weight of 44 g/mol (CO_2). In this case, special attention should be paid to the presence of an effect at 645°C on the ion current curve for the removal of a gaseous substance with a molecular weight of 18 g/mol (H_2O), which indicates the removal of H_2O molecules from sample **3**, represented by single strongly bonded OH groups, from the sample composite structure located randomly in the sample structure [34–36].

Figure 5 shows the SEM and TEM images of sample **3**. When a homogeneous suspension based on GO and Mt is treated with ultrasound, the initial layered components are destroyed up to the nanoscale range, as evidenced by the TEM image (Fig. 5a). After co-precipitation of GO and Mt, the SEM image shows crystallized Mt particles 200 nm–3 μm in size coated with GO sheets (Figs. 5b, 5c). It should be noted that the interaction between GO and Mt is quite strong,

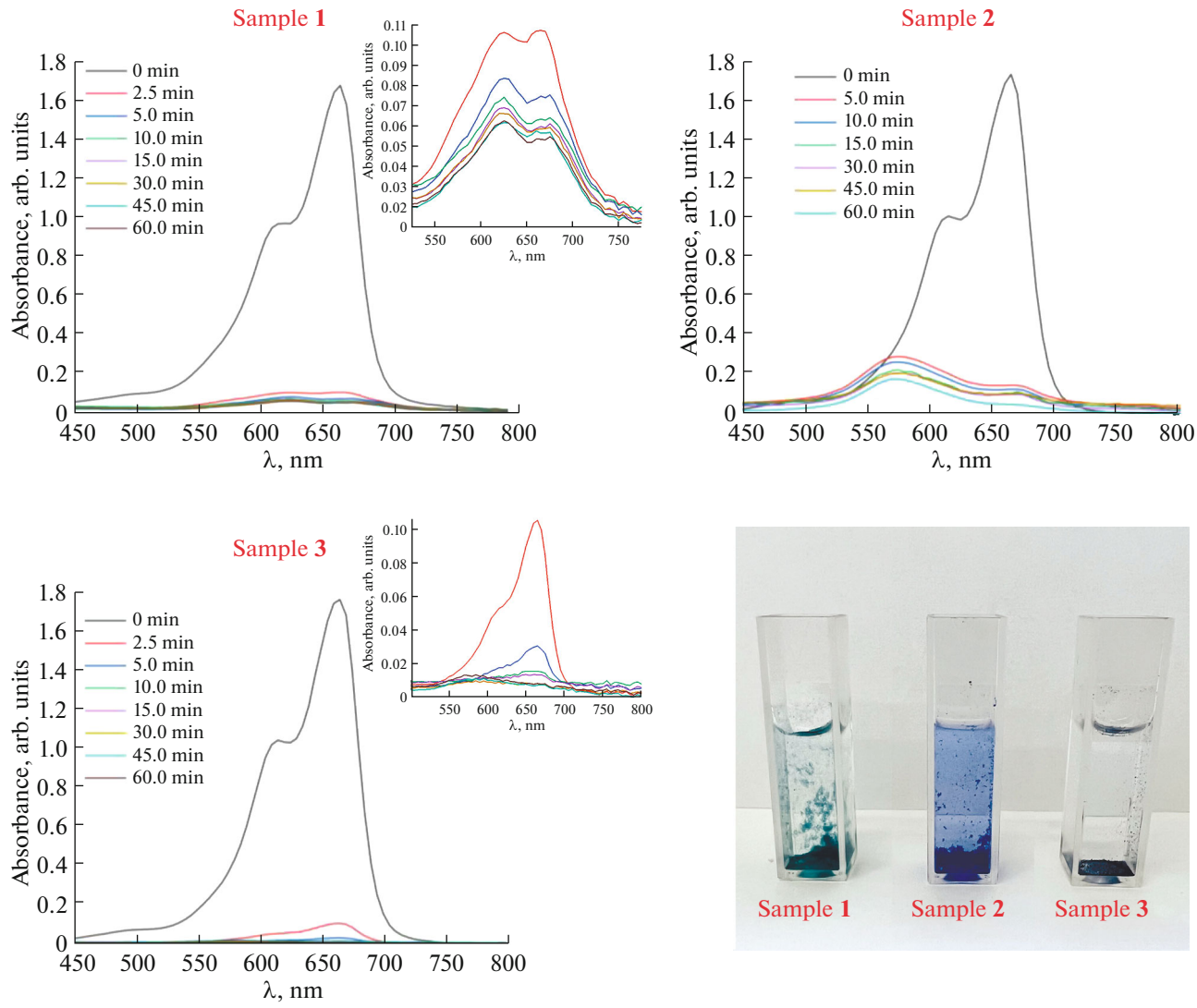

Fig. 6. Results of the study of the sorption of methylene blue by GO (sample **1**), Mt (sample **2**), a composite based on them (sample **3**) and a photograph of the experimental results.

since no destruction of the structure is observed during subsequent sonication. This interaction can be explained by the emerging van der Waals forces and the formation of coordination bonds between the GO surface and Mt.

To study the adsorption capacity of organic dyes both as individual components—graphene oxide (sample **1**) and montmorillonite (sample **2**) and as a composite based on them (sample **3**), methylene blue sorption from an aqueous solution was chosen (Fig. 6).

As is known [27, 40–42], graphene oxide and materials based on it are good sorbents for cationic dyes due to the surface rich in oxygen-containing functional groups. Figure 6 shows that graphene oxide (sample **1**) is capable of removing up to 90% of 10 ppm methylene blue within 5 min of vigorous stirring. However, complete removal of the dye from the aqueous system does not occur with vigorous stirring for 60 min. Montmorillonite (sample **2**) exhibits a similar sorption capacity for methylene blue. According to the obtained data and the presented sorption curves (Fig. 6), the composite based on GO and Mt (sample **3**) has a higher sorption capacity with respect to methylene blue than the previously studied samples **1** and **2**. The composite removes more than 90% of the dye in less than for 2.5 min of intensive stirring of methylene blue in an aqueous solution, and within 45 min, sample **3** completely adsorbs it from the solution. It should be noted that the synthesized composite has an obvious advantage over commercial Mt, which is a highly hydrophilic substance, and centrifugation is necessary after sorption to remove the sorbent. The synthesized composite based on GO and Mt (sample **3**) has a lower dispersibility in water due to the partial closure of oxygen-containing groups, which makes it possible to

separate the solution after sorption by simple filtration.

CONCLUSIONS

A new method for preparation of a composite based on graphene oxide and montmorillonite, which can act as an effective sorbent for the removal of methylene blue from an aqueous solution, is presented. The composite was studied by X-ray powder diffraction, IR and Raman spectroscopies, and SEM, indicating the presence of bonds between montmorillonite and graphene oxide in the composite structure. The above DTA/TG/DSC curves show the removal of internal interlayer water and oxygen-containing groups over a wide temperature range when heated to 1000°C. A comparative study of the adsorption of methylene blue (10 ppm) in the presence of a composite sample, as well as the initial components, was carried out. It was shown that the rate of dye adsorption on a composite based on GO and Mt is higher than on samples of graphene oxide or montmorillonite, which can be used in the development of new materials and coatings for the sorption of harmful substances in various industries.

ACKNOWLEDGMENTS

The authors thank A. F. Korotkov for help with synthetic experiments. X-ray diffraction studies were performed using the equipment of the Center for Collective Use of the Physical Methods of Investigations at the Kurnakov Institute of General and Inorganic Chemistry, Russian Academy of Sciences. Scanning electron microscopy was carried out using the equipment of the Educational and Methodological Center for Lithography and Microscopy of the Moscow State University.

FUNDING

This work was supported by the Russian Science Foundation (project no. 22-19-00110).

CONFLICT OF INTEREST

The authors declare that they have no conflicts of interest.

REFERENCES

1. P. Luo, W. Liu, D. Zhu, et al., Colloids Surf., A: Physicochem. Eng. Asp. **655**, 130216 (2022). https://doi.org/10.1016/j.colsurfa.2022.130216
2. A. Alkenani and T. A. Saleh, J. Mol. Liq. **367**, 120291 (2022). https://doi.org/10.1016/j.molliq.2022.120291
3. B. Mustafa, T. Mehmood, Z. Wang, et al., Chemosphere **308**, 136333 (2022). https://doi.org/10.1016/j.chemosphere.2022.136333
4. K. S. Lakshmy, D. Lal, A. Nair, et al., Polymers **14**, 1604 (2022). https://doi.org/10.3390/polym14081604
5. G. P. Panasyuk, I. V. Kozerozhets, E. A. Semenov, et al., Inorg. Mater. **55**, 929 (2022). https://doi.org/10.1134/S0020168519090139
6. A. N. Tarasova, J. Int. Pharm. Res. **12**, 1169 (2020). https://doi.org/10.31838/ijpr/2020.SP2.142
7. N. Makisha, Membranes **12**, 819 (2022). https://doi.org/10.3390/membranes12090819
8. A. Kiselev, E. Magaril, D. Panepinto, et al., Sustainability **13**, 12885 (2022). https://doi.org/10.3390/su132212885
9. M. E. A. Ali, A. Shahat, T. I. Ayoub, et al., Biointerface Res. Appl. Chem. **12**, 7556 (2022). https://doi.org/10.33263/BRIAC126.75567572
10. O. A. Butusova, J. Int. Pharm. Res. **12**, 1156 (2020). https://doi.org/10.31838/ijpr/2020.SP2.140
11. S. Raj, H. Singh, and J. Bhattacharya, Sci. Total Environ. **857**, 159464 (2023). https://doi.org/10.1016/j.scitotenv.2022.159464
12. M. K. Chow, C. E. Jee, and S. P. Yeap, Results Eng. **16**, 100682 (2022). https://doi.org/10.1016/j.rineng.2022.100682
13. N. A. Bulychev, Nanosci. Technol. **12**, 91 (2021). https://doi.org/10.1615/NanoSciTechnolIntJ.2021038033
14. A. Memetova, I. Tyagi, P. Singh, et al., J. Clean. Prod. **379**, 134770 (2022). https://doi.org/10.1016/j.jclepro.2022.134770
15. R. Liu, S. Gao, Q. Peng, et al., Fuel **330**, 125567 (2022). https://doi.org/10.1016/j.fuel.2022.125567
16. N. Jahan, H. Roy, A. H. Reaz, et al., J. Environ. Chem. Eng. **6**, 100239 (2022). https://doi.org/10.1016/j.cscee.2022.100239
17. I. Kozerozhets, G. Panasyuk, A. Semenov, et al., Powder Technol. **413**, 118030 (2023). https://doi.org/10.1016/j.powtec.2022.118030
18. G. P. Panasyuk, I. V. Kozerozhets, E. A. Semenov, et al., Inorg. Mater. **55**, 920 (2019). https://doi.org/10.1134/S0020168519090127
19. E. I. Senkina, A. S. Buyakov, S. O. Kazantsev, et al., Coatings **12**, 1107 (2022). https://doi.org/10.3390/coatings12081107
20. O. V. Bakina, E. A. Glazkova, A. S. Lozhkomoev, et al., Cellulose **25**, 4487 (2018). https://doi.org/10.1007/s10570-018-1895-z
21. A. Zhang, J. Liu, Y. Yang, et al., Chem. Eng. J. **451**, 138762 (2023). https://doi.org/10.1016/j.cej.2022.138762
22. A. Nkwoada, G. Oyedika, E. Oguzie, et al., Inorg. Chem. Commun. **143**, 109768 (2022). https://doi.org/10.1016/j.inoche.2022.109768
23. H. Yang, M. Li, L. Pan, et al., Environ. Res **216**, 114423 (2023). https://doi.org/10.1016/j.envres.2022.114423
24. S. O. Akpotu, P. N. Diagboya, I. A. Lawal, et al., Chem. Eng. J. **216**, 114423 (2023). https://doi.org/10.1016/j.cej.2022.139771

25. S. Nehra, A. Dhillon, R. Sharma, et al., Environ. Nanotechnol. Monit. Manage. **18**, 100690 (2022). https://doi.org/10.1016/j.enmm.2022.100690

26. J. Song, S. Zhang, G. Li, et al., J. Hazard. Mater. **391**, 121692 (2020). https://doi.org/10.1016/j.jhazmat.2019.121692

27. A. Molla, Y. Li, B. Mandal, et al., Appl. Surf. Sci. **464**, 170 (2019). https://doi.org/10.1016/j.carbon.2019.10.003

28. A. C. Reynosa-Martinez, G. N. Tovar, W. R. Gallegos, et al., J. Hazard. Mater. **384**, 121440 (2020). https://doi.org/10.1016/j.jhazmat.2019.121440

29. Y. V. Ioni, S. I. Chentsov, I. V. Sapkov, et al., Russ. J. Inorg. Chem. **67**, 1711 (2022). https://doi.org/10.1134/S0036023622601076

30. W. S. Hummers and R. E. Offeman, J. Am. Chem. Soc. **80**, 6 (1958). https://doi.org/10.1021/ja01539a017

31. X. Zhang, H. Yi, H. Bai, et al., RSC Adv. **7**, 41471 (2017). https://doi.org/10.1039/c7ra07816a

32. Y. V. Ioni, Y. A. Groshkova, S. P. Gubin, et al., Nanotechnol. Russ. **15**, 163 (2020). https://doi.org/10.1134/S1995078020020111

33. Z. Yang, Z. Yuan, Z. Shang, et al., Appl. Clay Sci. **197**, 105781 (2020). https://doi.org/10.1016/j.clay.2020.105781

34. I. Kozerozhets, G. Panasyuk, E. Semenov, et al., Ceram. Int. **48**, 7522 (2022). https://doi.org/10.1016/j.ceramint.2021.11.296

35. I. Kozerozhets, G. Panasyuk, E. Semenov, et al., Ceram. Int. **46**, 28961 (2020). https://doi.org/10.1016/j.ceramint.2020.08.067

36. I. V. Kozerozhets, G. P. Panasyuk, E. A. Semenov, et al., Russ. J. Inorg. Chem. **65**, 1384 (2020). https://doi.org/10.1134/S0036023620090090

37. K. A. Block, A. Trusiak, A. Katz, et al., Appl. Clay Sci. **107**, 173 (2015). https://doi.org/10.1016/j.clay.2015.01.021

38. Y. V. Ioni, Y. A. Groshkova, E. Y. Buslaeva, et al., Russ. J. Inorg. Chem. **66**, 950 (2021). https://doi.org/10.1134/S0036023621060115

39. S. Yang, Q. Chen, M. Shi, et al., Nanomaterials **10**, 770 (2020). https://doi.org/10.3390/nano10040770

40. Z. Danková, A. Mockovčiaková, and S. Dolinská, Desalin. Water Treat. **52**, 28 (2014). https://doi.org/10.1080/19443994.2013.814006

41. A. S. Kuzenkova, A. Y. Romanchuk, A. L. Trigub, et al., Carbon (2019). https://doi.org/10.1016/j.carbon.2019.10.003

42. H. Yan, X. Tao, Z. Yang, et al., J. Hazard. Mater. **268**, 191 (2014). https://doi.org/10.1016/j.jhazmat.2014.01.015

Translated by V. Avdeeva